Alqalam Journal of Medical and Applied Sciences. 2025;8(2):581-595
https://doi.org/10.54361/ajmas.258208

Original article

Scale Effect on the Behavior of Geotextile-Reinforced Soil Under Square Footing

Khowla Imbark*, Enas Altalhe

Department of Faculty of Civil and Structural Engineering, Omar Almukhtar University, Albyda, Libya
Corresponding Email. *enas.omer@omu.edu.ly*

Abstract
The present research investigates how footing width affects the geotextile-reinforced clay soil's bearing capability. A numerical simulation of footing width was used to examine how bearing capacity changes with width, and several laboratory experiments were conducted to investigate how footing width affects the behavior of reinforced soil. The results display that as footing width increases, so does the load bearing capacity; this effect was most pronounced between 80 and 250 mm, after which there was little difference in the bearing capacity settlement curves. Depending on the reinforcement ratio R_r, the impact of the bearing capacity ratio in reinforced soil may vary as the footing width changes. The BCR barely changed when the footing width was changed at Rr of 4. The models with larger footing widths had a higher BCR than those with smaller footing widths at reinforcement ratios below 4. BCR values for smaller model scales were higher for reinforcement ratios larger than 4.
Keywords. Scale Effect, Bearing Capacity, Square Footing, Reinforcement Ratio, Clay Soil.

Introduction

The most widely used material for construction is soil, and it sometimes has insufficient engineering attributes. In this regard, several scholars are continuously trying to come up with fresh approaches to enhance the features. The technology known as geosynthetic reinforced soil (GRS) foundation treatment has become popular in the building, railroad, highway, and other engineering domains. The GRS foundation has the potential to significantly minimize the footing's settlement and enhance its loading capacity.

Numerous researchers have looked into how well geosynthetic reinforced soil foundations perform under footing load. Several simulations were conducted to look into the load-settlement response of GRS foundations under strip footing, circular footing, square footing, rectangular footing, and ring footing. Together with experimental research, numerical modelling was employed to verify model test results and examine the impact of different influencing factors on GRS foundation performance [1-4]. Numerous studies have been carried out to develop an appropriate system in terms of expense and efficiency employing geosynthetic components enhances the foundations' ability to support loads. While some of these investigations have focused on embedded footing, others have examined surface footing conditions. These studies have used various types, numbers of geosynthetic layers, and other parameters that may affect the ultimate bearing capacity 5-**Error! Reference source not found.**15].

To investigate the improvement in bearing capacity, Omer et al. [16] employed small-scale simulations with square and strip footings on sand foundation strengthened by geogrid layers. They came to the following conclusions: the depth of the initial layer, u, is less than B; the maximum BCR at layer width is approximately 8B for strip footing and 4.5B for square footing; and the depth of layers required to reach the maximum BCR is roughly 2B for strip footing and 1.4B for square footing. Shirazi et al [**Error! Reference source not found.**17] was reviewed previous studies were reviewed to show the benefits of the soil-bearing ability of a bio-based geotextile for weak soil foundation. He found that the topmost layer's spacing, the vertical distance between layers, the quantity of reinforcement layers, and the layer length are the most crucial factors that increase bearing capacity. The maximum increase in bearing capacity was attained with a length layer ratio of up to three, and the ideal number of layers was suggested to be three to four. Das et al. [18] compare the ability to enhance the load-bearing capacity of strip foundations on geogrid-strengthened sand and clay. They do this by conducting a model test with variable parameters, such as the depth of the initial layer of the geogrid (u) in sand and saturated clay in series, both the depth and width of the reinforcing layers (h, L), and other variables. This allows them to compare and identify the ideal parameters that result in the maximum increase. They discover that the ultimate load settlement of a foundation on reinforced and unreinforced clay is roughly the same, but in sand, reinforcement causes the ultimate load to rise along with the foundation's settlement (the sand-geogrid system's bearing enhancement was greater than that of a clay-geogrid system). The geogrid's depth for its highest ultimate bearing capacity was approximately 2B in sand and 1.75B in clay, while the initial layer of geogrid was at a depth of 0.3B to 0.4B with an ideal width of 8B in sand and 5B in clay.

As observed by Cerato [19], genuinely model-scale footing test results produced larger values of N_γ than theoretical formulas because model-scale footing tests were utilised to determine the majority of bearing capacity factors. As a result, they should not be used for full-scale footing design without a decrease. Thus, the relationship between N_γ and footing dimensions may be directly related to the average stress felt beneath a footing; the larger the footing, the greater the mean stress and the smaller the friction angle. This could

Received*: 18-02-2025 -* ***Accepted****: 07-04-2025 -* ***Published****: 13-04-2025*

be related to the curvature of the Mohr–Coulomb failure encompass. Understanding the behaviour of both reinforced and unreinforced soil that emerged beneath the shallow foundations required a thorough grasp of the scale effect. Fakher and Jones [**Error! Reference source not found.**] demonstrated that failing to account for the scale effect in reinforced soils will result in unsuitable results, and thus, the reinforcement mechanism has not been evaluated in actual situations. They demonstrated that, using dimensional analysis, they concluded that the stiffness of encouragement in test models should be $1/n^2$ times that of the encouragement used in the field, where n is the ratio of the footing width in the field to that in model tests. Das and Omar [**Error! Reference source not found.**] investigated the scale effect by varying the footing width. The examiners concluded that increasing the footing width may raise the failure load as well as lowering its capacity for bearing ratio (BCR), which is the ratio of the bearing capacity of the reinforced soil foundation to that of the unreinforced soil solution.

This paper investigated the scale effect of reinforced soil foundations. As key component of real field design is the bearing capacity ratio, and scale effect describes the behavioural differences between field observations and model tests. In the present investigation, the soil's load-bearing capacity beneath a square footing with B=250 was investigated. To test the same cases for B=150mm, B=250mm was utilised. A numerical test was performed on one of these cases, and an experimental and numerical test was conducted on the other for verification.

Materials

Soil

The soil utilised in this investigation was gathered from Shahat-libya; Table 1, to depth 0.7m, the soil sample was dried under room temperature for month (air dried 25°C ±5), after that, the important physical and mechanical properties that describe and classified the soil were carried out following American Society of Testing Materials (ASTM) specification. After drying, the soil was aggregated to larger particles, so it had to be washed in sieves no.4 and 200 to calculate the retaining percentage of soil. The R4 and R200 were found to be 8.94% and 32.114%, respectively. The ASTM D-2487 uniform classification of fine-grained inorganic soil was used to classify soil, with soft soil classified as CL (group symbol)-Sandy lean clay (group name).

Table 1. Details of soil sample used for testing.

Sample marking		**Soil sample**
Location		Shahat- Libya
Coordinates	**Latitude**	32.822362
	Longitude	21.869251
Water content w (%)		15.17
Sample condition		Disturbed
Depth of soil collected		0.7 m
Field density		1.792 g/cm^3

Table 2. Most important mechanical and physical properties of used soil.

Soil properties			**25±5°C**	**ASTM test designation**
Consistency limits	LL (%)		32.947	D4318-17
	PL (%)		19.036	
	PI (%)		13.911	
Specific Gravity Gs			2.553	D854-98
Compaction	Max. dry density ϒd (g/cm3)		1.825	D698-91
	O.W.C (%)		14.831	
Hydrometer analysis	Silt (%)		77.3	D422-63
	Clay (%)		29.5	
Unconfined compression test, qu (kg/cm3)	Dry case		17.726	D-2166
	Wet case		2.679	
CBR (%)	Soaked soil	2.5mm	8.694	D-1883
		5mm	7.728	
	Unsoaked soil	*2.5mm*	*14.877*	
		5mm	13.782	
Direct shear test	Cohesion (KN/m3)		53.66	D3080-03
	Angle of friction (°)		48	

Received*: 18-02-2025 -* ***Accepted****: 07-04-2025 -* ***Published****: 13-04-2025*

The chosen soil was a soft dark green clay have a 32.947 % liquid limit and 19.036% plastic limit. It was discovered that the specific gravity was 2.553. According to a standard Procter test, the ideal dry density was 1.825 g/cm^3, and the optimal water content was 14.831%. Table 2 provides additional properties.

Geotextile

In this study, a pair of geotextile types will use: woven and nonwoven textile as shown in Figure. 1. A geotextile has a Fabric weight of 250 g/m2 for woven and 400 g/m2 for nonwoven and nonwoven geotextile was used with thickness 3.8 mm under 2KN/m2 and its grab elongation >100%. An axial stiffness, EA, was 2000 KN/m for woven and 2135.2 KN/m for nonwoven geotextile. The manufacturer's information sheet provided the reinforcement's mechanical and physical characteristics which are displayed in Table 3.

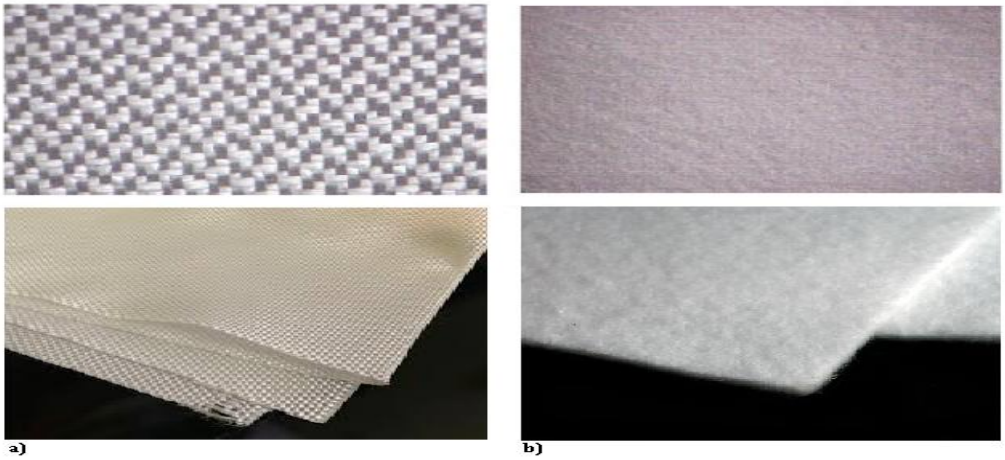

Figure 1. Geotextile used in this study, a) woven-geotextile, b) nonwoven-geotextile.

Table 3. Engineering properties of geotextiles.

Property	Nonwoven textile		Woven textile
Fabric weight (g/m2)	400		250
Thickness (mm)	3.8		-
tensile strength (N)	Grab tensile strength (M.D) (N)	1000	1068
	Grab tensile strength (C.D) (N)	1750	
Permeability (cm/s)	0.25		0.04
Transmissivity (L/M/H)	220		-

Footing

The test was conducted using a square footing model made of 15*15 and 25*25 cm steel plates with 25 mm thickness, on a center of footing surface a hole was created and a rod of diameter similar to the diameter of the bearing rod was installed for applying load as shown in Figure.2, the footings have axial stiffness and bending stiffness of 750000KN/m and 39.06KNm2/m for B=150mm and 125000 KN/m and 65.10 KNm2/m for B=250mm, respectively.

Experimental data

The laboratory equipment mainly consisted of a tank, a rectangular steel footing, and a loading device. Chummar [22] states that the soil failure surface stretches from the footing's edge by about 2B on each side and has a depth of about 1.1B from the base of the foundation. To minimise the effects of ends, the box was made of a steel tank with dimensions of 1.6×1×m and a depth of 0.5m. One of the test tank walls was made of 5 mm-thick polycarbonate glass, supported directly on two steel columns. To prevent lateral deformation, the exterior of the sides of the tank were supported by steel columns, and the interior walls of the box were polished to lessen friction with the ends of the foundation. In order to endure plane strain conditions, the tank box was designed to be sufficiently rigid. A hydraulic jack welded to A response frame was employed for placing the load on the footing, and a dial gauge with a 200KN capacity was used to measure the applied load, with load increases implemented and sustained until the settlement s/B rate hit sixteen percent. Two dial gauges on the footing side were used to measure the settlement. The setup of the model footing is shown in Figure 3.

Received*: 18-02-2025 -* ***Accepted****: 07-04-2025 -* ***Published****: 13-04-2025*

Figure 2. Models of the footing used in this study.

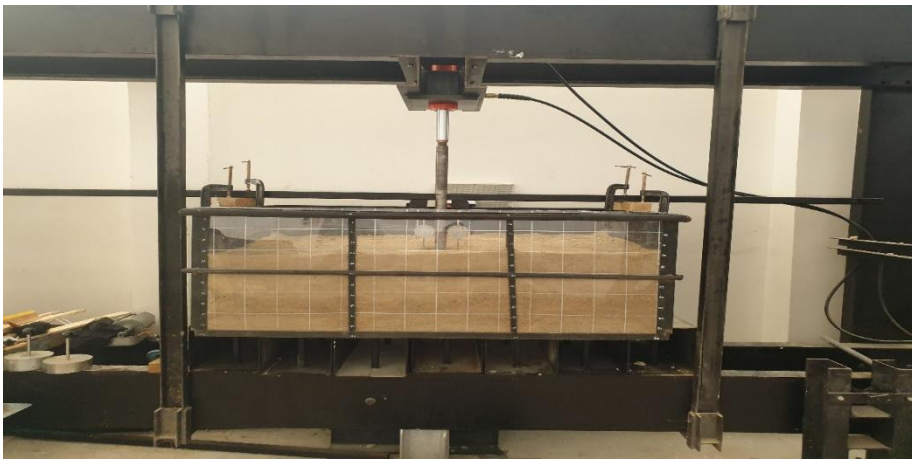

Figure 3. Model footing load test arrangement in the laboratory.

Table 4 shows two series of tests, each with a different B value. Each experiment used a 9.5mm sieve to ensure soil homogeneity. The water was then added according to the test program and mixed by hand, the box was covered with four layers of soil, each of which was between 100 and 150 mm thick, A 15 mm diameter steel plate weighing 8 kg was used to level and compact the soil after the amount of soil needed for each layer was established. The number of blows ranged from 25 to 50 times the desired density. Until the soil reaches the required depth of 500 mm, this process is repeated for every layer, after which it is covered for at least 24 hours to ensure uniform moisture distribution. To avoid eccentric loading, the foundation was precisely centered on the loading jack, and the surface was levelled once the final layer was completed. A hydraulic jack was used to load the footing, which was supported by the reaction frame. The load transmitted to the footing was measured with a load gauge and gradually applied. The dry density was 1.23±0.05 g/cm3, achieving 68±3% of the highest dry density of soil. The soil's moisture content was calculated as 8.24±1%. The ratio of soil depth to footing width ranged from 2 to 2.6.

Table 4 shows that the experimental cases Wr3-25, Wr6-25, Wr9-25, Wr12-25, Nr3-25, Nr6-25, Nr9-25, and Nr12-25 cannot be tested experimentally because the geotextile's dimension is greater than the test box's width. Therefore, the other experimental model was repeated using finite element analysis by Plaxis 2D to model the experimental models with a longer width of the test box to include the effect of L/B=8. The hardening soil HS model can be used to simulate stress-displacement behavior in soil modelling. Conclusions of the experimental and numerical analyses agree well, so we can rely on them for cases where L/B = 8.

In addition to the two footing widths mentioned earlier, other footing widths (B= 80mm, 350mm, and 450mm) were numerically studied in this research to understand how the loading bearing capacity of unreinforced soil changes.

Table 4. Experimental Test Program for Reinforced Soil.

No. of test	Reinforcement type	U/B	L/B	B (cm)	No. of test	Reinforcement type	U/B	L/B	B (cm)
Ur1	Without	-	-		**-**	-	-	-	
Wr1-25	Woven geotextile	0.25	3	25	**Nr1-25**	Non-woven geotextile	0.25	3	25
Wr1-15				15	**Nr1-15**				15
Wr2-25	Woven geotextile	0.25	6.67	25	**Nr2-25**	Non-woven geotextile	0.25	6.67	25
Wr2-15				15	**Nr2-15**				15

Received*: 18-02-2025 -* ***Accepted****: 07-04-2025 -* ***Published****: 13-04-2025*

Wr3-25	Woven geotextile	0.25	8	25	**Nr3-25**	Non-woven geotextile	0.25	8	25
Wr3-15				15	**Nr3-15**				15
Wr4-25	Woven geotextile	0.3	3	25	**Nr4-25**	Non-woven geotextile	0.3	3	25
Wr4-15				15	**Nr4-15**				15
Wr5-25	Woven geotextile	0.3	6.67	25	**Nr5-25**	Non-woven geotextile	0.3	6.67	25
Wr5-15				15	**Nr5-15**				15
Wr6-25	Woven geotextile	0.3	8	25	**Nr6-25**	Non-woven geotextile	0.3	8	25
Wr6-15				15	**Nr6-15**				15
Wr7-25	Woven geotextile	0.67	3	25	**Nr7-25**	Non-woven geotextile	0.67	3	25
Wr7-15				15	**Nr7-15**				15
Wr8-25	Woven geotextile	0.67	6.67	25	**Nr8-25**	Non-woven geotextile	0.67	6.67	25
Wr8-15				15	**Nr8-15**				15
Wr9-25	Woven geotextile	0.67	8	25	**Nr9-25**	Non-woven geotextile	0.67	8	25
Wr9-15				15	**Nr9-15**				15
Wr10-25	Woven geotextile	1	3	25	**Nr10-25**	Non-woven geotextile	1	3	25
Wr10-15				15	**Nr10-15**				15
Wr11-25	Woven geotextile	1	6.67	25	**Nr11-25**	Non-woven geotextile	1	6.67	25
Wr11-15				15	**Nr12-15**				15
Wr12-25	Woven geotextile	1	8	25	**Nr12-25**	Non-woven geotextile	1	8	25
Wr12-15				15	**Nr12-15**				15

Results

The two series of tests have been conducted as mentioned before for a square footing with width =150mm and for a square footing with width =250mm. According to before process, the findings of these model evaluations are summarized in Table 4 for B= 150mm and 250mm, respectively. In this Table, the BCRs obtained at settlement ratios s/B= 16% are presented.

Table 5. Summary of Model Tests for 150mm and 250 mm footing widths

Test No.	Geotextile Type	u mm	L mm	s/B=16%		Test No.	Geotextile Type	u mm	L mm	s/B=16%	
				q KN/m^2	BCR					q KN/m^2	BCR
Ur1-15	-	-	-	491.06	-	**Ur1-25**	-	-	-	626.85	-
Wr1-15	Woven	37.5	450	800	1.63	**Wr1-25**	Woven	62.5	750	535.52	0.85
Wr2-15	Woven	37.5	1000	768.40	1.56	**Wr2-25**	Woven	62.5	1666	907.43	1.45
Wr3-15	Woven	37.5	1200	1104.66	2.25	**Wr3-25**	Woven	62.5	2000	553.29	0.88
Wr4-15	Woven	45	450	610.76	1.24	**Wr4-25**	Woven	75	750	483.63	0.77
Wr5-15	Woven	45	1000	552.11	1.21	**Wr5-25**	Woven	75	1666	802.49	1.28
Wr6-15	Woven	45	1200	1211.45	2.39	**Wr6-25**	Woven	75	2000	388.48	0.62
Wr7-15	Woven	100	450	800	1.63	**Wr7-25**	Woven	167.5	750	881.28	1.41
Wr8-15	Woven	100	1000	803.95	1.64	**Wr8-25**	Woven	167.5	1666	1091.35	1.74
Wr9-15	Woven	100	1200	758.62	1.54	**Wr9-25**	Woven	167.5	2000	1761.64	2.81
Wr10-15	Woven	150	450	680.96	1.39	**Wr10-25**	Woven	250	750	763.16	1.22
Wr11-15	Woven	150	1000	537.54	1.09	**Wr11-25**	Woven	250	1666	910.75	1.45
Wr12-15	Woven	150	1200	551.11	1.13	**Wr12-25**	Woven	250	2000	773.92	1.23
Nr1-15	Non-woven	37.5	450	956.26	1.95	**Nr1-25**	Non-woven	62.5	750	545.33	0.87
Nr2-15	Non-woven	37.5	1000	660.22	1.34	**Nr2-25**	Non-woven	62.5	1666	894.15	1.43
Nr3-15	Non-woven	37.5	1200	572.07	1.16	**Nr3-25**	Non-woven	62.5	2000	434.84	0.69
Nr4-15	Non-woven	45	450	702.22	1.39	**Nr4-25**	Non-woven	75	750	415.45	0.66
Nr5-15	Non-woven	45	1000	766.67	1.56	**Nr5-25**	Non-woven	75	1666	1057.04	1.69
Nr6-15	Non-woven	45	1200	421.62	0.86	**Nr6-25**	Non-woven	75	2000	247.98	0.40
Nr7-15	Non-woven	100	450	800	1.63	**Nr7-25**	Non-woven	167.5	750	919.11	1.47
Nr8-15	Non-woven	100	1000	674.05	1.37	**Nr8-25**	Non-woven	167.5	1666	918.07	1.46

Received*: 18-02-2025 -* ***Accepted****: 07-04-2025 -* ***Published****: 13-04-2025*

Nr9-15	Non-woven	100	1200	858.67	1.75	**Nr9-25**	Non-woven	167.5	2000	1878.18	3.00
Nr10-15	Non-woven	150	450	763.48	1.55	**Nr10-25**	Non-woven	250	750	854.08	1.36
Nr11-15	Non-woven	150	1000	552.27	1.12	**Nr11-25**	Non-woven	250	1666	1007.68	1.61
Nr12-15	Non-woven	150	1200	387.22	0.79	**Nr12-25**	Non-woven	250	2000	538.51	0.86

Effect of footing width

The load-bearing capability ratio is a crucial factor in real field design, and the scale effect refers to behavioral variations between field observations and model tests. [23]

The soil's bearing capacity beneath a square footing with B=250 was examined in the current investigation. B=250mm was used to test the identical cases for B=150mm. For verification, some of these cases underwent experimental and numerical testing, while others underwent numerical testing. Findings indicate that the second series' bearing capacity differs from the first series' bearing capacity. This difference is related to the arrangement of the reinforcement.

Effect of footing width for unreinforced soil

In this investigation, the load-settlement curves for B=150mm and 250mm were obtained experimentally and numerically, both experimental and numerical analyses showing a high degree of behavioural matching- as shown in Figure. 4. Three additional footing widths, 80mm, 350mm, and 450mm, were studied numerically in the unreinforced case to evaluate the scale effect on bearing capacity.

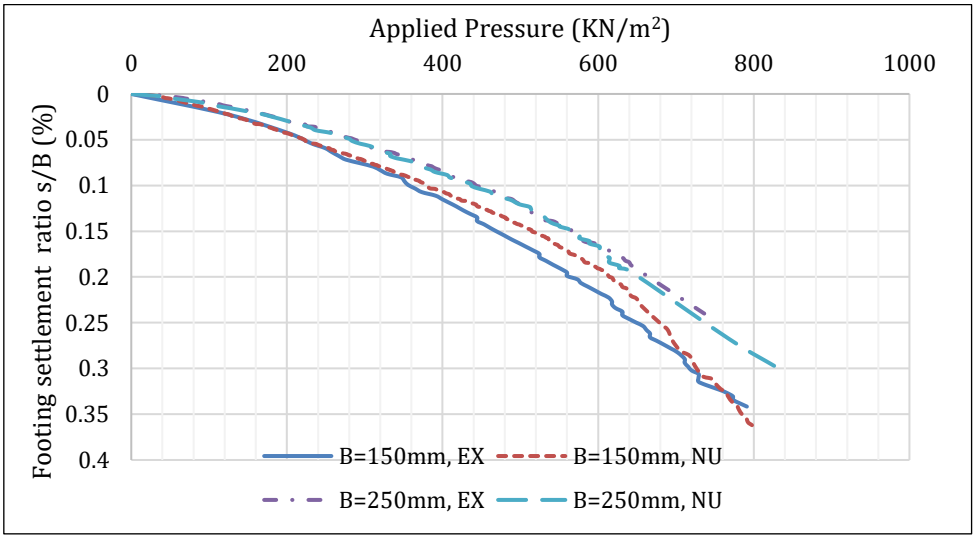

Figure 4. Comparison between experimental and numerical results for unreinforced foundation.

The same soil properties were identified in all cases. Figure 5 depicts the bearing capacity-settlement ratio for footings of different widths. The maximum capacity for bearing in this process was not reached because the test ran until the settlement ratio was 0.2B. The soil behaviour is elastic until s/B=0.01, at which point the settlement increases with the applied load, and the curves are non-linear elastic models. as the breaking point is unclear in these curves, the comparison will take place at a specific point of settlement.

The load-bearing capacity raises as the footing's width increases, as shown in Figure 5. The soil failure resembles punching shear failure at a smaller scale of footing B=80mm, but it resembles local shear failure at a larger scale.

So the mobilized shear strength depends on the footing width; this effect was most noticeable between 80 and 250mm width, after which the bearing capacity-settlement curves did not differ significantly. To validate these models, model tests on the response to bearing ability of footing width B were carried out experimentally and numerically with widths of 150mm and 250mm. For these two models, the numerical pressure-settlement curves match the results of the laboratory models, with minor differences due to soil, footing, and environmental conditions of plain strain; additionally, some other model tests were carried out. in numerical analysis.

In the interest of calibrating the results for both numerical and experimental analysis, the soil's final bearing capacity was confirmed using four equations: Hansen, Vesic, Mayerhoff, and Terzagi. Because the shape of the curves has changed, the q_{ult} in this section will be determined by the value of settlement obtained using the tangent intersection method, as shown in the Figure 6.

Received: *18-02-2025* - ***Accepted***: *07-04-2025* - ***Published***: *13-04-2025*

https://doi.org/10.54361/ajmas.258208

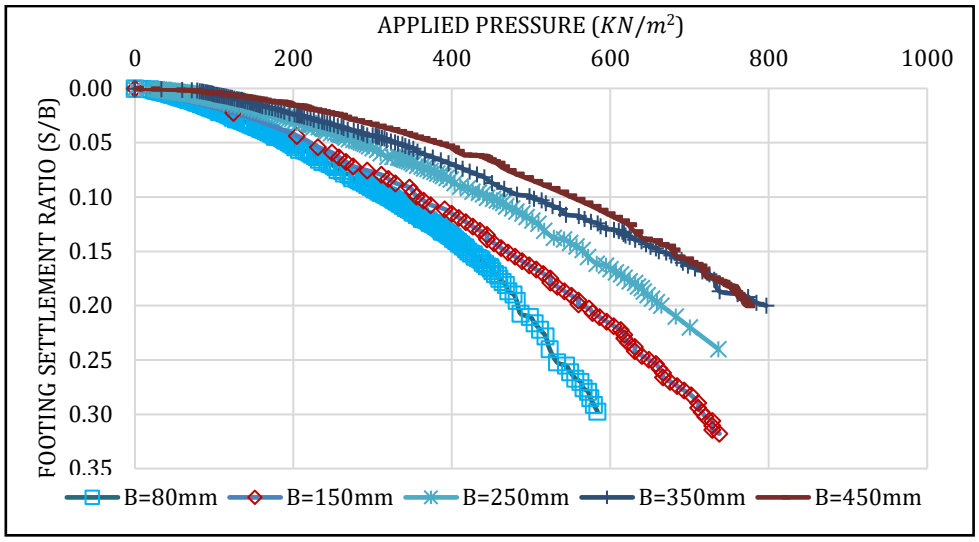

Figure 5. The unreinforced soil's bearing capacity of footings scale.

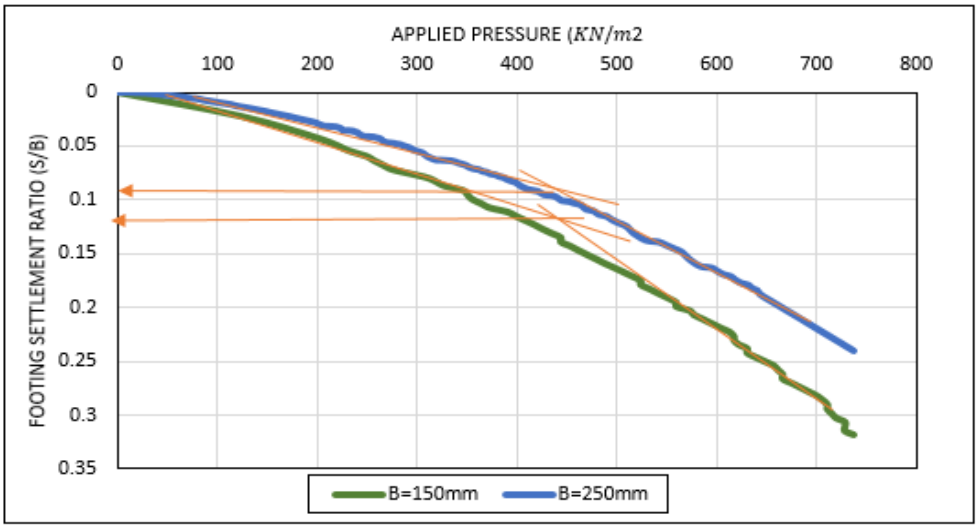

Figure 6. Determine the point of settlement change for B=150mm and 250mm curves.

Terzagi's general equation for soil bearing capacity in the context of square footing failure is as follows:

$q_u = 1.3CN_c + \gamma DN_q + 0.4\gamma BN_\gamma$

Where,N_c, N_q, N_γ are bearing capacity factors were provided by Terzaghi as soil friction angle functions, ∅.

The general Meyerhof equation that takes into account the inclined load factor (i_c, i_q, i_γ), the base shape factor (S_c, S_q, S_γ), and the depth coefficient (d_c, d_q, d_γ) is:

$q_u = CN_cS_cd_ci_c + \gamma DN_qS_qd_qi_q + 0.5\gamma BN_\gamma S_\gamma d_\gamma i_\gamma$

Vesic used the Hansen equation, which was developed by Meyerhof, to consider sloping soil, with the difference in the bearing capacity coefficient N_γ. So, they have the same equation with the same N_c and N_q and different N_γ, as:

$N_q = e^{\pi \tan \emptyset} \tan^2(45 + \frac{\emptyset}{2})$

$N_c = (N_q - 1)\cot \emptyset$

$N_\gamma = (N_q - 1)\tan(1.4\emptyset)$ For Meyerhof

$N_\gamma = 1.5(N_q - 1)\tan(\emptyset)$ For Hansen

$N_\gamma = 2(N_q + 1)\tan(\emptyset)$ For Vesic

Each method includes a table that identifies the bearing capacity factors related to angle friction. In this work, there were no loading inclinations, the footing type was square, and the footing depth was zero, so the related coefficients were cancelled. The results of four methods for footing with B=150mm and 250mm at s/B=0.125 and 0.095, respectively, are summarized in Table (4-7) and Figure (4-31).

A strong correlation with the Vesic, Meyerhof, and Hansen methods can be observed in Table 4-7. The reason why Terzagi's bearing capacity was greater than others could be that, according to Terzagi's formula, soil is

Received: *18-02-2025* - ***Accepted***: *07-04-2025* - ***Published***: *13-04-2025*

https://doi.org/10.54361/ajmas.258208

a rigid, perfectly plastic substance that unexpectedly fails when it reaches its bearing capacity. The following equation describes how bearing capacity changes with footing width:
q_u = 0.0473B + 433.27

Table 6. Final bearing capacity for numerical, physical, and theoretical computations for unreinforced case.

Method	q_u (KN/m2)			
	B=150mm	Δq^*(%)	B=250mm	Δq^*(%)
Terzagi	461.53	2.93	465.60	1.58
Meyerhof	433.90	3.23	438.39	4.34
Hansen	437.11	2.51	439.30	4.14
Vesic	439.23	2.04	442.82	3.38
Experimental	422.03	5.87	426.16	7.01
Plaxis	448.39	0	458.32	0

$^*\Delta q = (q_u - q_{plaxis}/q_{plaxis}) * 100$

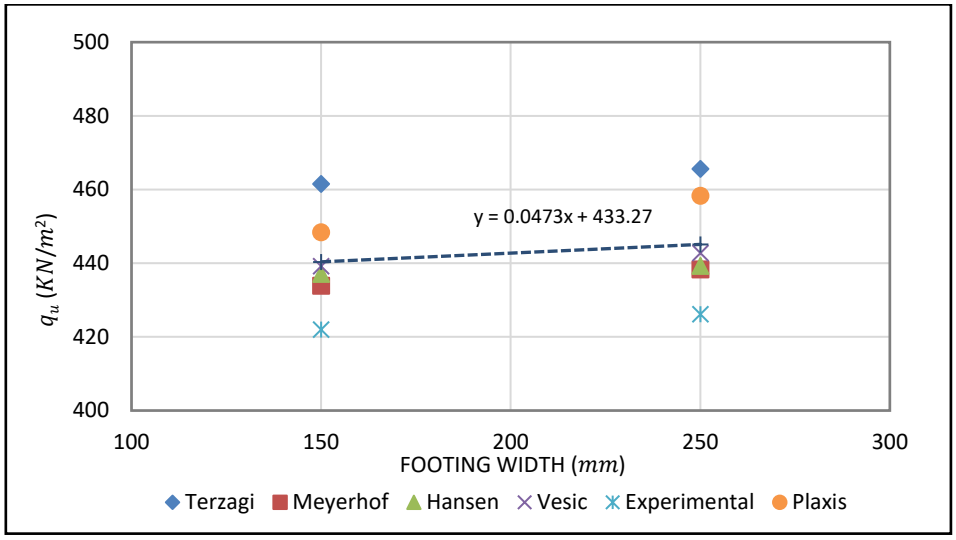

Figure 7. The change in bearing capacity with footing width effect of footing width for reinforced soil

According to Terzagi's theory, increasing the footing width causes the failure zones to become more extensive, which increases the foundation's bearing capacity. As noted by Das and Omer [**Error! Reference source not found.**], Faker and Jones [20], and Chen and Abu-Farsakh [**Error! Reference source not found.**], BCR values for small-scale models may overestimate reinforcement advantages. To find out how well model footing tests perform in comparison to real full-scale footings on reinforced soil foundations, larger footing widths were compared to smaller ones.
This effect appears stronger on coarse-grained soil than on fine-grained soil, as stated in the literation, due to the larger particle size. Because the soil in this study contains considerable amounts of sand and silt particles, this effect could be significant.

Effect of footing width on reinforcement top spacing and length
Because the maximum bearing capacity in the case without reinforcement for footings B=150 mm and B=250mm was at different points of settlement, the behaviour of the two footings will be compared at specific settlement/width ratios (s/B= 16%) as display in Table. 5, in additional to another point of settlement (s/B= 5%); it is clear that, in most cases, the BCR values are similar or decrease at B=250mm compared to B=150mm footing. However, in some cases, these values increase. Figures. 8 through 11 show the BCR values versus u/B at various geotextile lengths for both footing widths at settlement ratios s/B=5% and 16%.
In both woven and non-woven geotextiles, the settlement rate ratio (s/B) is 5%, Figures 8 and 9, the BCRs values are almost identical in most cases, particularly for small values of u and L. The scale effect became more noticeable as the geotextile length increased, peaking at L/B=8. As the settlement ratio increases, so do the changes in BCR values.

Received: *18-02-2025* - ***Accepted***: *07-04-2025* - ***Published***: *13-04-2025*

a)

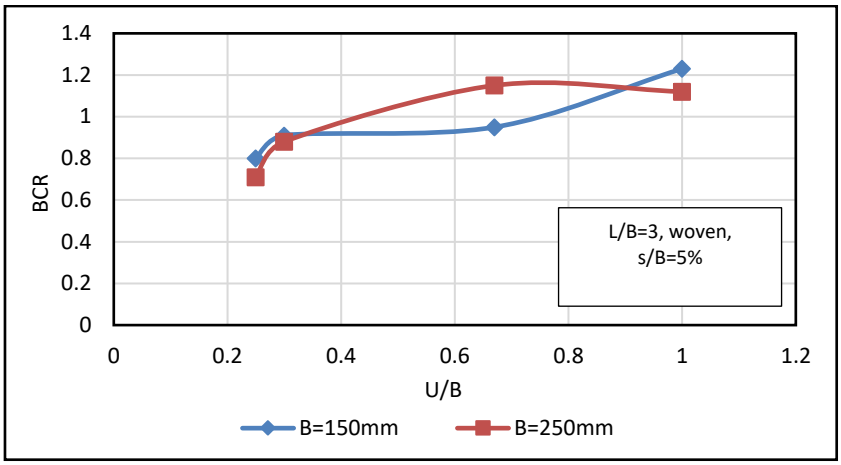

b)

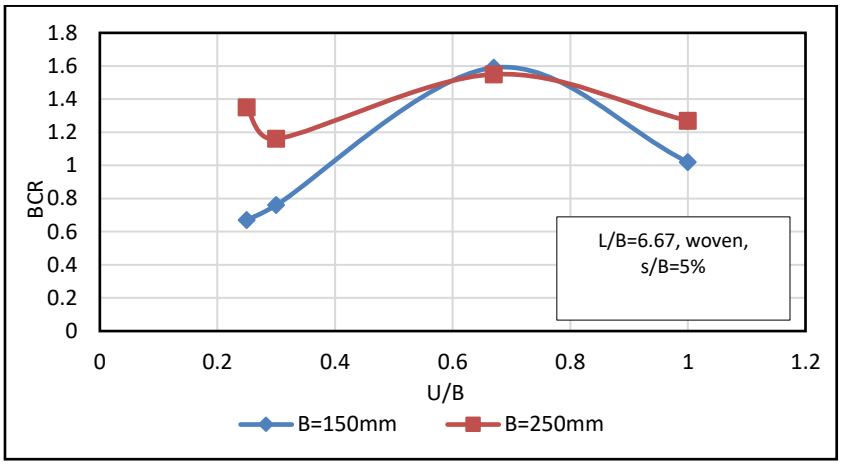

c)

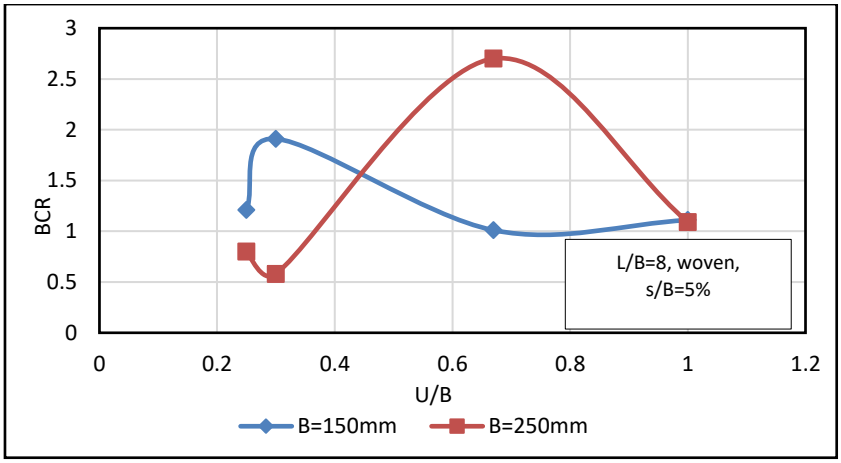

Figure 8. Effect of reinforcement spacing with various lengths of woven geotextile at settlement ratio s/B= 5% , a) For L/B=3, b) For L/B=6.67, c) For L/B=8.

a)

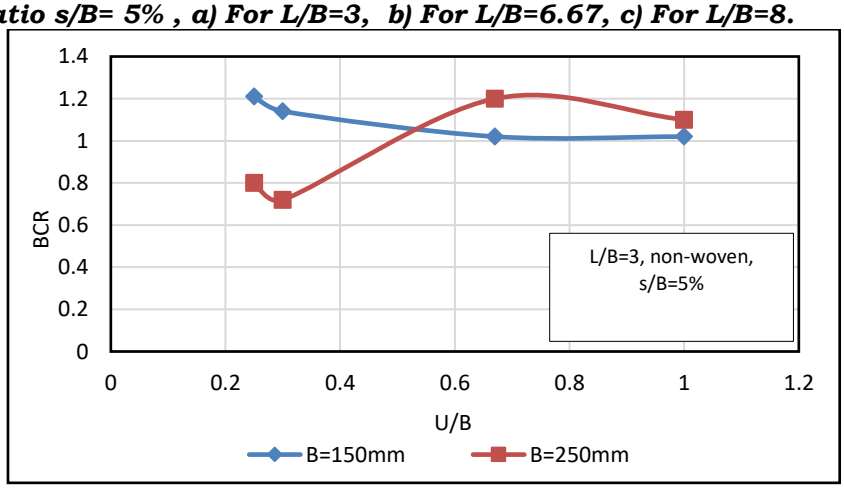

Received: *18-02-2025* - ***Accepted***: *07-04-2025* - ***Published***: *13-04-2025*

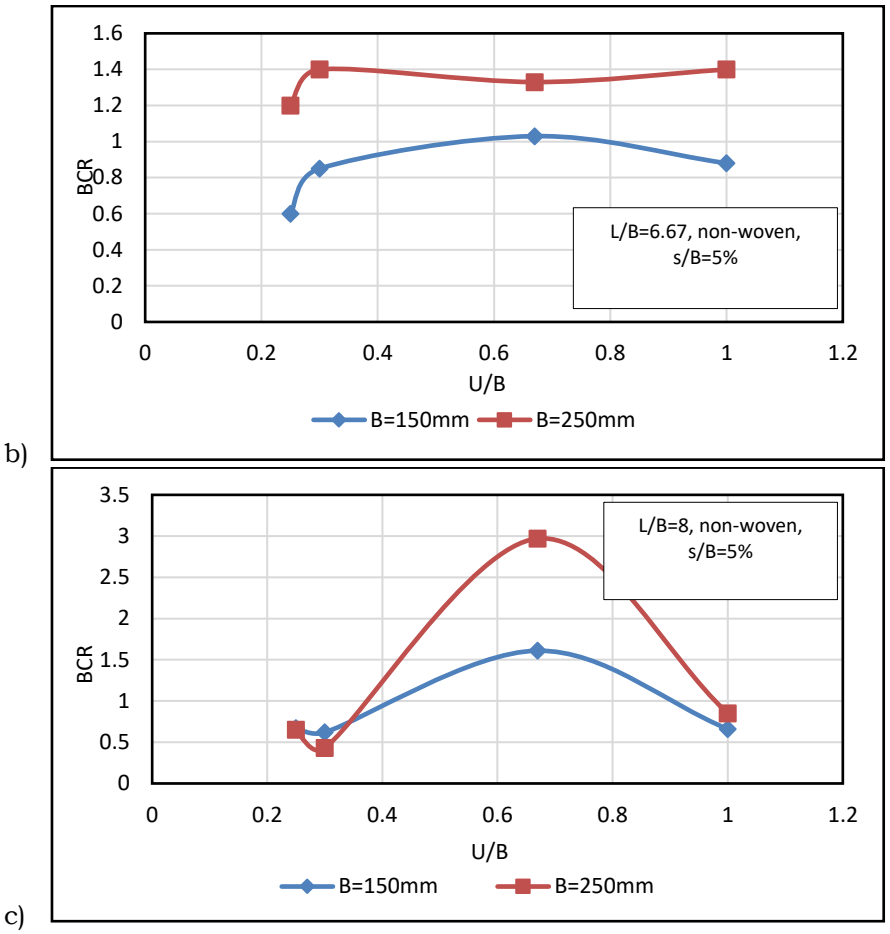

Figure 9. Effect of reinforcement spacing with various lengths of non-woven geotextile at settlement ratios s/B= 5%, a) For L/B=3, b) For L/B=6.67, c) For L/B=8.

Figures 10 and 11 display the BCR values for both footing widths at s/B=16%. For L/B=8, at two footing widths, the ideal value of u/B was found to be u/B=0.25 and 0.67, which could be attributed to the mobilized tensile strength and increased obvious cohesion caused by increased L. This finding corresponds to Ahmad et al [25].

Footing width had a greater impact on woven geotextile because the interaction of soil particles with it increased. The BCR value at L/B=8 of footing width B=250mm was reduced up to u/B=0.3, then increased to u/B=0.67. At u/B=1, the BCR values remained constant in all cases, indicating that the effect of scale was minimal. According to Ahmad et al. [25]. The greatest amount of strain along the reinforcement occurs just beneath the footing center and decreases as the distance from the footing center increases. As a result, the reinforcement length may additionally impact the reinforced soil's performance. In all previous cases, it is clear that, numerous factors affect how the footing width affects the behavior of reinforced soil. As mentioned earlier, there are situations where the change in BCR with footing width is small, and other situations where it is large.

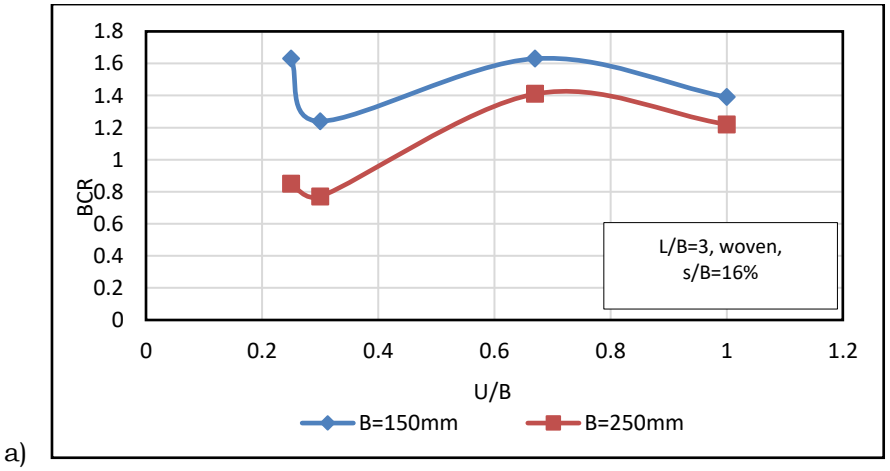

Received: *18-02-2025* - ***Accepted***: *07-04-2025* - ***Published***: *13-04-2025*

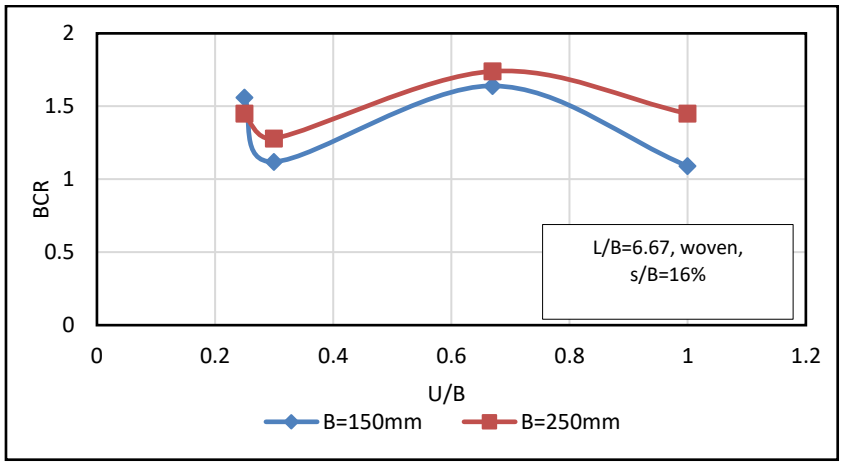

b)

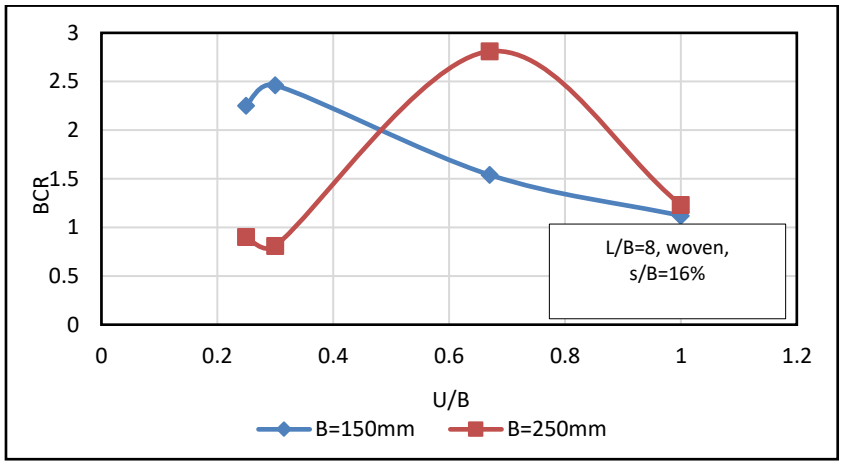

c)

Figure 10. Effect of reinforcement spacing with various lengths of woven geotextile at settlement ratios s/B= 16%, a) For L/B=3, b) For L/B=6.67, c) For L/B=8.

This observation is related to the quantity and placement of reinforcement in the soil. In addition, the impact of reinforcement strength and the reciprocal response between geotextile and soil. In addition to the differences in Young's modulus values between laboratory tests, all of these factors influence these conclusions. Thus, according to Chen et al. [**Error! Reference source not found.**], the scale influence mainly correlates with the reinforced region's reinforced ratio (R_r), which can be written as follows:

$$R_r = \frac{E_R * A_R}{E_S * A_S}$$

Where:

E_R : The reinforcement's modulus of elasticity, $E_R = J/t_R$; J symbolizes the reinforcement tensile modulus, t_R is the reinforcement thickness.

A_R : the area of reinforcement per unit width.

E_S : the soil's elasticity modulus.

A_S : the area of reinforced soil per unit width=d ×1; d is the overall depth of reinforced zone=u+(N−1)h.

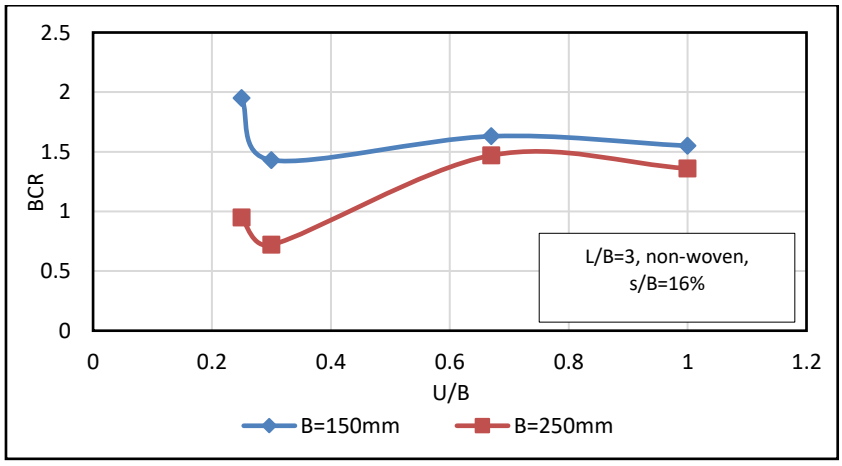

a)

Received: *18-02-2025* - ***Accepted***: *07-04-2025* - ***Published***: *13-04-2025*

b)

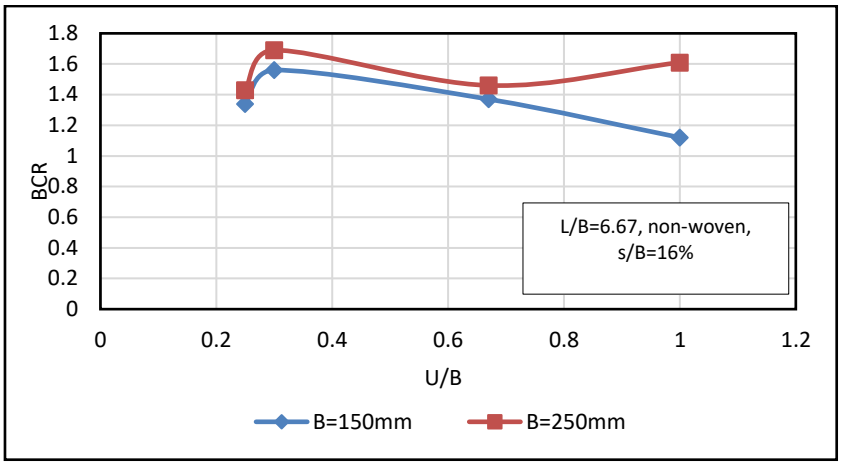

c)

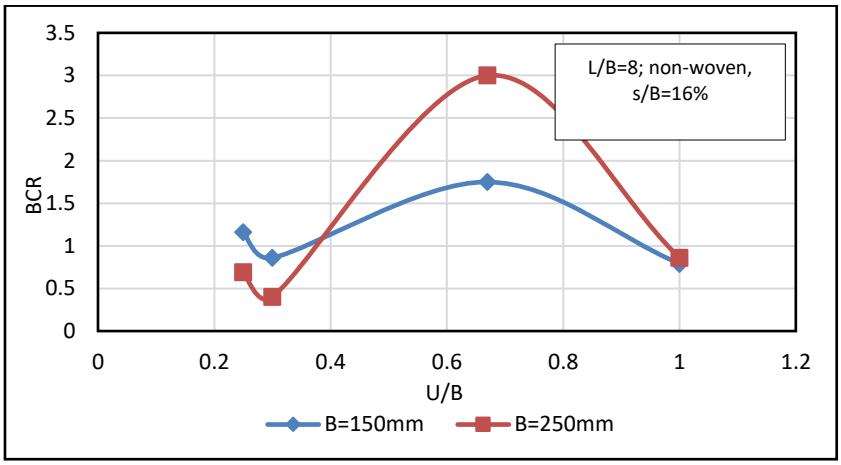

Figure 11. Effect of reinforcement spacing with various lengths of non-woven geotextile at settlement ratios s/B= 16%, a) For L/B=3, b) For L/B=6.67, c) For L/B=8.

The reinforcement ratio R_r was calculated for each test model, and as shown in the Table. 7, the reinforcement ratio decreases with increasing footing width. For foundation models under the two footings, the rate of decrease remains constant between each model and its counterpart. As a result, a comparison will be made between the reinforcement ratio for models with a footing with B=150mm and the ratio of the BCR for models under the 150 footing to the BCR for models under the 250 footing (BCR_{150}/BCR_{250}). Finding out how reinforced soil behaves when the footing scale is altered is the aim of this comparison.
Table 8 and Figure 12 show that the effect of footing width on the behaviour of reinforced soil is determined by the soil's reinforcement ratio. As a result, the BCRs for soil models under Footing with B=150mm are greater than those for soil models under Footing with B=250 as the reinforcement ratio increases.

Table 7. Reinforcement ratios for model test.

No. of test	R_r (B=150)	No. of test	R_r (B=250)	ΔR_r^*	No. of test	R_r (B=150)	No. of test	R_r (B=250)	ΔR_r^*
Wr1-15	8.13	**Wr1-25**	4.88	1.666667	**Nr1-15**	9.70	**Nr1-25**	5.82	1.666667
Wr2-15	4.74	**Wr2-25**	2.85	1.666667	**Nr2-15**	5.93	**Nr2-25**	3.56	1.666667
Wr3-15	10.35	**Wr3-25**	6.21	1.666667	**Nr3-15**	8.21	**Nr3-25**	4.92	1.666667
Wr4-15	7.91	**Wr4-25**	4.74	1.666667	**Nr4-15**	8.89	**Nr4-25**	5.33	1.666667
Wr5-15	4.31	**Wr5-25**	2.59	1.666667	**Nr5-15**	5.93	**Nr5-25**	3.56	1.666667
Wr6-15	11.03	**Wr6-25**	6.62	1.666667	**Nr6-15**	8.89	**Nr6-25**	5.33	1.666667
Wr7-15	7.12	**Wr7-25**	4.25	1.675	**Nr7-15**	3.81	**Nr7-25**	2.27	1.675
Wr8-15	2.53	**Wr8-25**	1.51	1.675	**Nr8-15**	3.33	**Nr8-25**	1.99	1.675
Wr9-15	2.37	**Wr9-25**	1.42	1.675	**Nr9-15**	1.67	**Nr9-25**	1.00	1.675
Wr10-15	4.74	**Wr10-25**	2.85	1.666667	**Nr10-15**	4.44	**Nr10-25**	2.67	1.666667
Wr11-15	1.85	**Wr11-25**	1.11	1.666667	**Nr11-15**	2.42	**Nr11-25**	1.45	1.666667
Wr12-15	1.58	**Wr12-25**	0.95	1.666667	**Nr12-15**	2.99	**Nr12-25**	1.79	1.666667

* ΔR_r = R_r (for models test at B=150mm) - R_r (for models test at B=250mm)

Received: *18-02-2025* - ***Accepted***: *07-04-2025* - ***Published***: *13-04-2025*

At a reinforcement ratio of 4, changing the footing width resulted in negligible changes in the BCR. At reinforcement ratios less than 4, the models with higher footing widths had a higher BCR than those with smaller footing widths. For reinforcement ratios greater than 4, BCR values for smaller model scales were higher. Higher reinforcement ratios produce greater differences. The relation between the proportion of reinforcement and the variation in BCR values can be expressed using the following equation:
BCR_{150}/BCR_{250} = 0.2065 R_r + 0.2075.

Table 8. Changes in BCR values with reinforcement ratios.

No. of test	BCR_{150}	BCR_{250}	BCR_{150}/BCR_{250}	R_r	No. of test	BCR_{150}	BCR_{250}	BCR_{150}/BCR_{250}	R_r
Wr1	1.63	0.85	1.92	8.13	**Nr1**	1.95	0.87	2.24	9.70
Wr2	1.56	1.45	1.08	4.74	**Nr2**	1.34	1.43	1.00	5.93
Wr3	2.25	0.88	2.56	10.35	**Nr3**	1.16	0.69	1.68	8.21
Wr4	1.24	0.77	1.61	7.91	**Nr4**	1.39	0.66	2.11	8.89
Wr5	1.21	1.28	0.95	4.31	**Nr5**	1.56	1.69	1.00	5.93
Wr6	2.39	0.81	2.95	11.03	**Nr6**	0.86	0.4	2.15	8.89
Wr7	1.63	1.41	1.50	7.12	**Nr7**	1.63	1.47	1.11	3.81
Wr8	1.64	1.74	0.94	2.53	**Nr8**	1.37	1.46	0.94	3.33
Wr9	1.54	2.81	0.55	2.37	**Nr9**	1.75	3	0.58	1.67
Wr10	1.39	1.22	1.14	4.74	**Nr10**	1.55	1.36	1.14	4.44
Wr11	1.09	1.45	0.75	1.85	**Nr11**	1.12	1.61	0.70	2.42
Wr12	1.13	1.23	0.92	1.58	**Nr12**	0.79	0.86	0.92	2.99

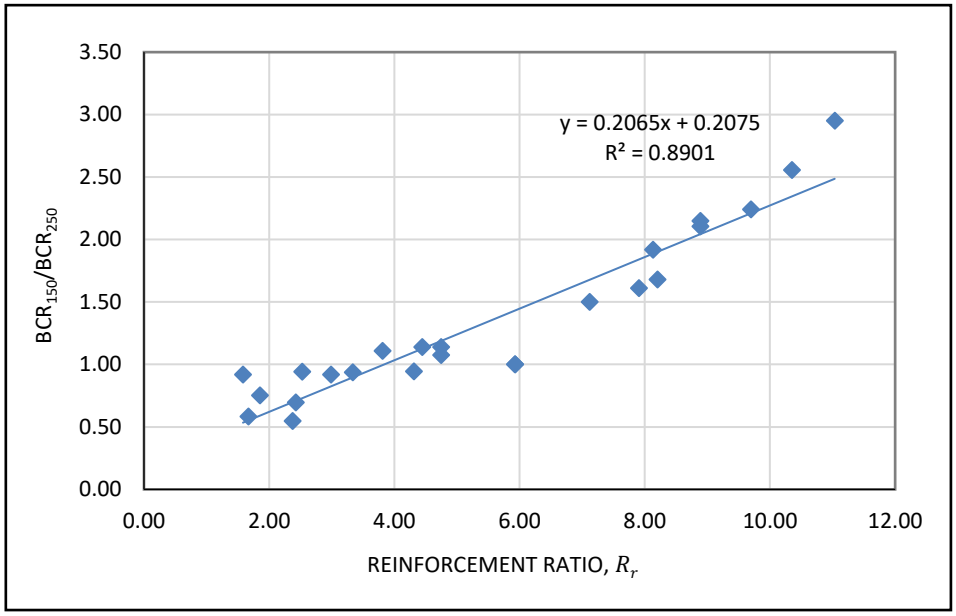

Figure 12. Relation between Rr and changes in BCRs.

Conclusion

In the current study, to determine the bearing capacity behaviour of a square footing placed on clay soil reinforced with geotextile, multiple lab experiments were conducted. The tests varied in length and depth of the layer, and the behaviour varied by type. As Field observations and model tests differ in behaviour; this is referred to as the scale effect. A critical consideration in real field design is the bearing capacity ratio, The current study investigated the bearing capacity of soil beneath a square footing with B=250. The identical cases for B=150mm were tested with B=250mm. In order to verify the findings, numerical testing was performed on one of these cases and experimental testing on the other. It is possible to draw the following conclusion: The soil's bearing capacity was raised by applying geotextile at different u/B and L/B ratios. The increasing width of the footing increases the bearing capacity; this was most noticeable between 80 and 250mm width, after which the bearing capacity-settlement curves did not differ significantly. The following equation describes how bearing capacity changes with footing width:

$$q_u = 0.0473B + 433.27$$

In reinforced soil, the effect of the bearing capacity ratio can change with the changing width of the footing according to the reinforcement ratio R_r. In comparison, the BCR for a footing width of 150mm to that for 250mm with reinforcement ratio, at R_r of 4, changing the footing width resulted in negligible changes in the

Received: *18-02-2025* - ***Accepted***: *07-04-2025* - ***Published***: *13-04-2025*

BCR. At reinforcement ratios less than 4, the models with higher footing widths had a higher BCR than those with smaller footing widths. For reinforcement ratios greater than 4, BCR values for smaller model scales were higher. Higher reinforcement ratios produce greater differences. The following equation may express the connection between the change in BCR values and the reinforcement ratio.

$$BCR_{150}/BCR_{250} = 0.2065\ R_r + 0.2075.$$

Conflict of interest. Nil

References

1. Omar MT, Das BM, Puri VK, Yen SC. Ultimate bearing capacity of shallow foundations on sand with geogrid reinforcement. Can Geotech J. 1993;30(3):545-9.
2. Basudhar PK, Saha Roy S, Deb K. Circular footings resting on geotextile-reinforced sand bed. Geotext Geomembr. 2007;25(6):377-84.
3. Latha GM, Somwanshi A. Effect of reinforcement form on the bearing capacity of square footings on sand. Geotext Geomembr. 2009;27(6):409-22.
4. Laman M, Yildiz A. Numerical studies of ring foundations on geogrid-reinforced sand. Geosynth Int. 2007;14(2):52-64.
5. Dash SK, Rajagopal K, Krishnaswamy N. Strip footing on geocell reinforced sand beds with additional planar reinforcement. Geotext Geomembr. 2001;19(8):529-38.
6. Dash SK, Rajagopal K, Krishnaswamy N. Behaviour of geocell-reinforced sand beds under strip loading. Can Geotech J. 2007;44(7):905-16.
7. Shin E, Das B, Lee E, Atalar C. Bearing capacity of strip foundation on geogrid-reinforced sand. Geotech Geol Eng. 2002;20:169-80.
8. Latha GM, Somwanshi A. Bearing capacity of square footings on geosynthetic reinforced sand. Geotext Geomembr. 2009;27(4):281-94.
9. Sireesh S, Sitharam T, Dash SK. Bearing capacity of circular footing on geocell-sand mattress overlying clay bed with void. Geotext Geomembr. 2009;27(2):89-98.
10. El Sawwaf M, Nazir AK. Behavior of repeatedly loaded rectangular footings resting on reinforced sand. Alexandria Eng J. 2010;49(4):349-56.
11. Tafreshi SM, Dawson A. Comparison of bearing capacity of a strip footing on sand with geocell and with planar forms of geotextile reinforcement. Geotext Geomembr. 2010;28(1):72-84.
12. Lovisa J, Shukla SK, Sivakugan N. Behaviour of prestressed geotextile-reinforced sand bed supporting a loaded circular footing. Geotext Geomembr. 2010;28(1):23-32.
13. Kazi M, Shukla SK, Habibi D. Behavior of embedded strip footing on sand bed reinforced with multilayer geotextile with wraparound ends. Int J Geotech Eng. 2015;9(5):437-52.
14. Kazi M, Shukla SK, Habibi D. Behaviour of an embedded footing on geotextile-reinforced sand. Proc Inst Civ Eng Ground Improv. 2016;169(2):120-33.
15. Shahin HM, Nakai T, Morikawa Y, Masuda S, Mio S. Effective use of geosynthetics to increase bearing capacity of shallow foundations. Can Geotech J. 2017;54(12):1647-58.
16. Omar M, Das B, Puri V, Yen S. Ultimate bearing capacity of shallow foundations on sand with geogrid reinforcement. Can Geotech J. 1993;30(3):545-9.
17. Shirazi MG, Rashid ASBA, Nazir RB, Rashid AHBA, Moayedi H, Horpibulsuk S, et al. Sustainable soil bearing capacity improvement using natural limited life geotextile reinforcement-A review. Minerals. 2020;10(5):479.
18. Das B, Shin E, Omar M. The bearing capacity of surface strip foundations on geogrid-reinforced sand and clay-a comparative study. Geotech Geol Eng. 1994;12:1-14.
19. Cerato AB, Lutenegger AJ. Scale effects of shallow foundation bearing capacity on granular material. J Geotech Geoenviron Eng. 2007;133(10):1192-202.
20. Fakher A, Jones CJ. Bearing capacity of rectangular footings on geogrid-reinforced sand. J Geotech Eng. 1996;122(4):326-7.
21. Das BM, Omar MT. The effects of foundation width on model tests for the bearing capacity of sand with geogrid reinforcement. Geotech Geol Eng. 1994;12:133-41.
22. Chummar AV. Bearing capacity theory from experimental results. J Soil Mech Found Div. 1972;98(12):1311-24.
23. Vesić AS. Analysis of ultimate loads of shallow foundations. J Soil Mech Found Div. 1973;99(1):45-73.
24. Chen Q, Abu-Farsakh M. Numerical analysis to study the scale effect of shallow foundation on reinforced soils. In: Geo-Frontiers 2011: Advances in Geotechnical Engineering. 2011. p. 595-604.
25. Ahmad H, Mahboubi A, Noorzad A. Scale effect study on the modulus of subgrade reaction of geogrid-reinforced soil. SN Appl Sci. 2020;2:1-22.
26. Chen Q, Abu-Farsakh MY, Sharma R, Zhang X. Laboratory investigation of behavior of foundations on geosynthetic-reinforced clayey soil. Transp Res Rec. 2007;2004(1):28-38.
27. Terzaghi K. Theoretical soil mechanics. 1943.
28. Meyerhof GG. The ultimate bearing capacity of foundations on slopes. In: Proc., 4th Int. Conf. on Soil Mechanics and Foundation Engineering. 1957. p. 384-6.
29. Hansen JB. A revised and extended formula for bearing capacity. 1970.

Received*: 18-02-2025 -* ***Accepted****: 07-04-2025 -* ***Published****: 13-04-2025*

https://doi.org/10.54361/ajmas.258208

الملخص

يهدف هذا البحث في التحقق من تأثير عرض الأساس على قدرة تحمل التربة الطينية المسلحة بالجيوتكستايل. استخدمت محاكاة عددية لعرض الأساس لدراسة كيفية تغير قدرة التحمل مع العرض، وأجريت العديد من التجارب المعملية لدراسة كيفية تأثير عرض الأساس على سلوك التربة المسلحة. تظهر النتائج أنه مع زيادة عرض الأساس، تزداد قدرة التحمل؛ وكان هذا التأثير أكثر وضوحا لعرض أساس بين 80 و250 مم، وبعد ذلك كان هناك فرق ضئيل في منحنيات قدرة التحمل ـ الهبوط. اعتمادا على نسبة التسليح Rr، قد يختلف تأثير نسبة قدرة التحمل في التربة المسلحة مع تغير عرض الأساس. بالكاد تغير BCR عند تغيير عرض الأساس عند Rr تساوي 4. كان للنماذج ذات عرض الأساس الأكبر BCR أعلى من تلك ذات عرض الأساس الأصغر عند نسب تسليح أقل من 4. كانت قيم BCR لمقاييس النماذج الأصغر أعلى لنسب التسليح الأكبر من 4.

Received*: 18-02-2025 -* ***Accepted****: 07-04-2025 -* ***Published****: 13-04-2025*